Proceedings of the Institute of Acoustics

SYNTHETIC APERTURE SONAR MOTION ESTIMATION USING NONLINEAR LEAST SQUARES

Daniel A. Cook, Daniel C. Brown, and Jose E. Fernandez
Code HS11
Naval Surface Warfare Center Panama City
110 Vernon Ave.
Panama City, FL 32407

1. INTRODUCTION

Synthetic aperture sonar (SAS) is the underwater acoustic counterpart to stripmap-mode synthetic aperture radar (SAR). Current seagoing SAS systems are deployed on unmanned robotic vehicles, commonly referred to as autonomous underwater vehicles (AUVs). As with SAR, SAS imaging is ideally done with a straight-line collection trajectory. However, SAS is far more susceptible to image degradation caused by the actual sensor trajectory deviating from a perfectly straight line. In fact, such unwanted motion is virtually unavoidable in the sea due to the influence of currents and wave action. In order to construct a perfectly-focused SAS image the motion must either be constrained to within one-eighth of a wavelength over the synthetic aperture, or it must be measured with the same degree of accuracy and then accounted for in the processing software. Since the former is not possible, the latter approach must be taken.

The technique known as redundant phase centers (RPC) has proven to be instrumental in solving the problem of SAS motion compensation. This paper will present an extension to the standard RPC technique[1,2] in which the time delays are decomposed into the components induced by the linear and angular velocities using nonlinear least squares to fit a model of the vehicle motion to the observed RPC time delays. Thus, the time delays observed in the image slant plane can be used to refine the motion estimate in an absolute frame of reference external to the AUV. The performance of this motion estimation scheme is shown using actual field data collected from a current US Navy research SAS system.

2. SAS PLATFORM MOTION

In this section we present, mainly for review, a simplified model of the ping-to-ping motion of the SAS sensor. It is assumed that the reader is familiar with the concepts of vernier arrays[3,4] and redundant phase centers[1,2] (also known as displaced phase centers). For the uninitiated, we provide the following rather unmotivated definitions: (1) A vernier SAS array comprises a single projector and multiple receivers. By applying a deterministic time delay correction to each channel, the vernier array is made to be equivalent to an array composed of elements each of which transmit and receive independently. (It is the assumption that each element both transmits and receives that forms the basis for the majority of mathematical synthetic aperture models.) The resulting 'virtual' elements are called phase centers and are located midway between the physical transmit and receive elements, as shown in Figure (1). (2) The term 'redundant phase centers' in the context of SAS imaging refers to the practice of timing the ping rate of the sensor such that one or more of the aftmost channels of the current ping overlap with the same number of the foremost channels of the previous ping. These overlapping channels will observe the same signals except for a time delay that is caused by orientation or motion error. Figure (2)

The authors gratefully acknowledge the US Office of Naval Research for its support of this work.

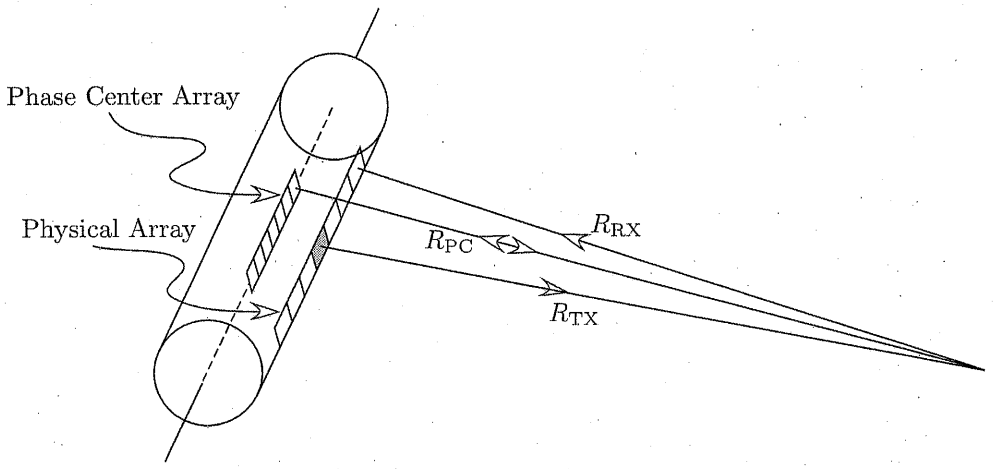

Figure 1: The physical array (a single projector and multiple receivers) can be replaced conceptually by an array of phase centers, each of which acts as a single transmit/receive pair. The shaded element represents the physical projector as well as a receiver.

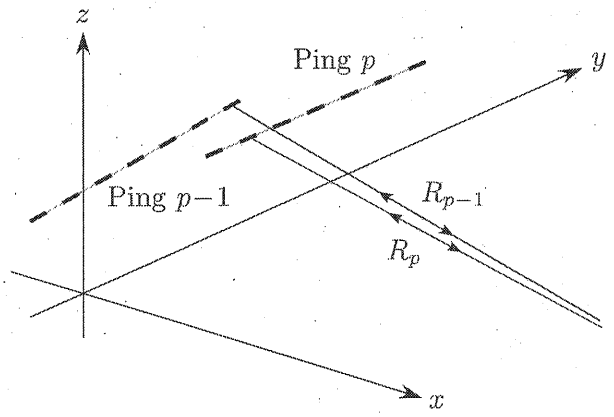

Figure 2: Overlapping a portion of the array from one ping to the next leads to overlapping phase centers that can be used to measure the time delays needed for motion estimation.

illustrates the concept. Clearly the time delays depend on the location of scatterers on the sea floor.

The delays from the redundant phase centers of the SAS vernier array can be measured and used to compensate for the unwanted platform motion. The time delay measurements are made by cross-correlating the signals from an RPC pair using a sliding window of relatively short duration. At each window position we obtain the time delay $\Delta\tau$ and the correlation coefficient ρ. Referencing Figure (3) (which is a cross-section of Figure (2)), the time delay is given by:

$$\begin{aligned}\Delta\tau &= 2\Delta R/c \\ &= \frac{2}{c}(R_p - R_{p-1}) \\ &= \frac{2}{c}\left(\sqrt{(x+\Delta x)^2+(z+\Delta z)^2} - \sqrt{x^2+z^2}\right),\end{aligned} \tag{1}$$

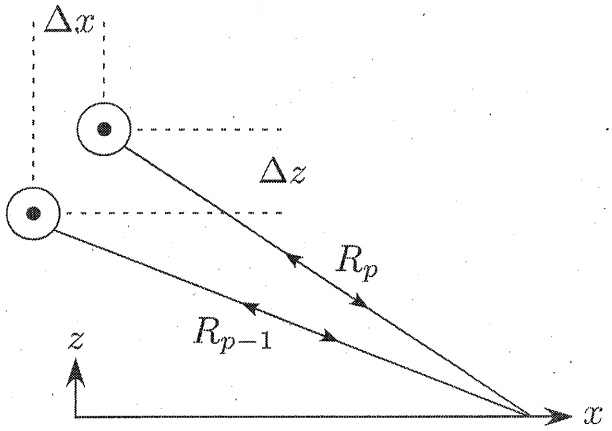

Figure 3: A cross-section in the x–z plane of a pair of redundant phase centers. When the stop-and-hop assumption is made, Δx and Δz do not vary with time.

where the subscript p is the ping number index. In this work, we will assume that the sea floor is a horizontal plane. If bathymetric information is available (from an interferometric array, for example), it can be incorporated in a straightforward manner into (1). It is also assumed that the RPC pair channels overlap perfectly in the y direction (no surge error).

3. MOTION ESTIMATION SCHEME

This section outlines the use of nonlinear least squares (NLLS) to find the vector $d = [\Delta x\ \Delta z]^{\mathrm{T}}$. The solution is Newton's method and is described in Chapter 10 of Dennis[5]. For a given RPC pair, $M > 2$ estimates of the time delay are typically available resulting in an overdetermined system of nonlinear equations. In the solution, we will need several quantities. First, we require the *residual function* which is what we seek to minimize. Its m^{th} entry is given by the difference between the estimated ($\Delta\hat{\tau}_m$) and measured ($\Delta\tau_m$) time delays:

$$D_m = \Delta\hat{\tau}_m - \Delta\tau_m, \tag{2}$$

where there are M measured RPC time delays and the vector $D \in \mathbb{R}^{M\times 1}$. The residual function is computed using the current estimate of d. Next we need the first derivative of D, which is the Jacobian matrix, $J \in \mathbb{R}^{M\times 2}$, where $J_{mn} = \partial D_m/\partial d_n$. Here, the m-index represents the m^{th} observed time delay and n indexes over the two components of d. The m^{th} row of J is

$$J_{m*} = \left[\frac{2(x+\Delta x)}{\sqrt{(x+\Delta x)^2+(z+\Delta z)^2}}\ \frac{2(z+\Delta z)}{\sqrt{(x+\Delta x)^2+(z+\Delta z)^2}}\right]. \tag{3}$$

The rows of the matrix J are evaluated using known quantities and the current guess for d. Next we require the second-derivative matrix, or the Hessian $\nabla^2 D_m \in \mathbb{R}^{2\times 2}$, of the m^{th} component of D where the matrix:

$$\nabla^2 D_{m,ij} = \frac{\partial^2 D_m(d)}{\partial d_i \partial d_j}. \tag{4}$$

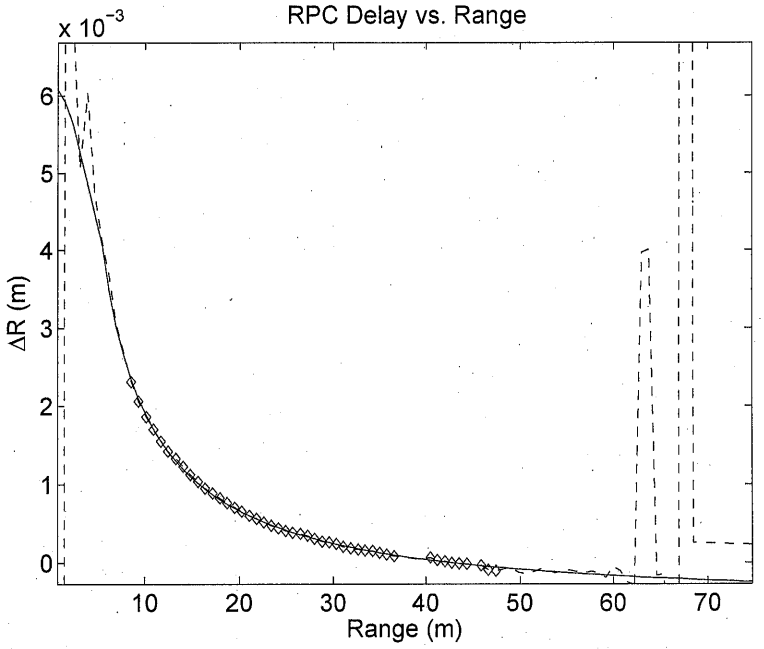

Figure 4: The plot above shows the typical performance of the nonlinear least squares technique. The broken line shows the measured RPC time delays as a function of range, and diamonds indicate the points used to estimate $[\Delta x \;\; \Delta z]^{\mathrm{T}}$ via nonlinear least squares where the correlation threshold was set to 0.9. The solid line shows the time delay as a function of range as computed using the estimated $[\Delta x \;\; \Delta z]^{\mathrm{T}}$.

is evaluated with the same information used to compute the Jacobian matrix. Based on (1), the Hessian matrix is:

$$\nabla^2 D_{m,ij} = \begin{bmatrix} \frac{2}{\hat{R}_p^2} - \frac{2(x+\Delta x)^2}{\hat{R}_p^3} & -\frac{2(x+\Delta x)(z+\Delta z)}{\hat{R}_p^3} \\ -\frac{2(x+\Delta x)(z+\Delta z)}{\hat{R}_p^3} & \frac{2}{\hat{R}_p^2} - \frac{2(z+\Delta z)^2}{\hat{R}_p^3} \end{bmatrix}, \tag{5}$$

where $\hat{R}_p = \sqrt{(x+\Delta x)^2 + (z+\Delta z)^2}$ is comupted using the current estimate of d. Lastly, let us define the quantity $S \in \mathbb{R}^{2\times 2}$:

$$S = \sum_{m=1}^{M} D_m \cdot \nabla^2 D_m. \tag{6}$$

Using all of the above, Newton's method applied to the nonlinear least squares problem is written as:

$$d^+ = d - \left(J^{\mathrm{T}} J + S\right)^{-1} J^{\mathrm{T}} D, \tag{7}$$

where d^+ is the updated estimate of d computed from the previous estimate or initial guess. Eq. (7) is iterated until the norm of the residual is below a specified threshold:

$$\|D\| = \left[D^{\mathrm{T}} D\right]^{1/2} < \epsilon_{\mathrm{tol}}.$$

Once this condition is met, the iteration stops and an estimates for the x and z components of the phase center displacement are obtained.

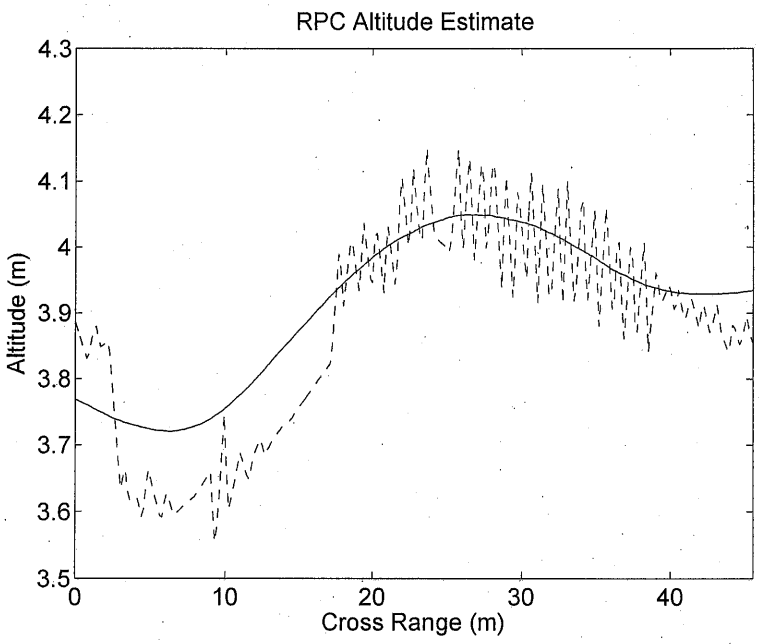

Figure 5: The interping heave (Δz) estimate has been integrated to yield an estimate of the altitude history for a segment of SAS12 data (solid line). The broken line shows the altitude measured by the on-board navigation system.

A practical refinement can be introduced into the solution (7) by weighting the entries of D by the cross-correlation coefficents. Let these coefficients be represented by the vector w and by the matrix W which is all zeros except for w appearing along the main diagonal. The weighted least-squares solution then becomes:

$$d^{+} = d - \left(J^{\mathrm{T}} W J + S\right)^{-1} J^{\mathrm{T}} W D, \tag{8}$$

where we must also change S:

$$S = \sum_{m=1}^{M} w_m D_m \cdot \nabla^2 D_m. \tag{9}$$

A simple strategy is to place a threshold on w such that the entries beneath say, 0.9, are set to zero. Thus, unreliable time delay estimates are effectively discarded and the solution is based only on the best measurements available. Figure (4) shows an example of the nonlinear least squares technique applied to field data from the SAS12 system sponsored by the US Office of Naval Research. The center frequency of this research sonar is 180kHz making the wavelength equal to 8.33mm. Note that the total variation of the observed RPC time delays is less than a single wavelength over the 70m swath shown in the plot. It is clear that the NLLS scheme does an excellent job of estimating the model parameters.

At this point, we have only estimated the interping displacement of one element in an RPC pair. This displacement can be caused by translations (sway, surge, heave) and rotations (pitch, roll, yaw). The final step in the motion estimation is to resolve the measured $d = [\Delta x \ \Delta z]^{\mathrm{T}}$ into translational and rotational components. In practice, current AUVs are outfitted with good-quality angular sensors so we assume the rotations are known from these. It is then a simple

matter to subtract the rotational contribution from $[\Delta x \ \Delta z]^{\mathrm{T}}$ yielding the desired sway and heave estimates. Figure (5) shows the integrated NLLS heave estimate compared to the altitude as recorded by the AUV's navigation computer. The constant of integration was chosen so that the mean of the NLLS curve coincides roughly with the mean of the measured altitude. Figure (6) shows a SAS image produced (a) without motion compensation and (b) using the NLLS technique.

4. CONCLUSION

We have presented a technique for extending the standard RPC SAS motion estimation that is capable of accurately resolving the measured RPC time delays into motions expressed in an external frame of reference. The resulting sway and heave estimates obtained from the nonlinear least squares RPC could potentially be used to improve the AUV's navigation while submerged. The simplified NLLS technique presented here is straightforward to implement and quite robust provided the RPC correlations are good. Another version is given by Cook[6] which dispenses with the stop-and-hop approximation and considers continuous motion of the array.

The present NLLS motion estimation assumes no error in the cross range direction (surge). In cases for which the SAS ping timing experiences substantial error, the RPC correlation values may drop to unacceptably low levels. A scheme to measure surge is given in a companion paper by Oeschger[7]. It could be used to properly align the RPC channels via interpolation prior to carrying out the NLLS motion estimation.

References

1. A. Bellettini and M. A. Pinto, "Theoretical accuracy of synthetic aperture sonar micronavigation using a displaced phase-center antenna," *IEEE Journal of Oceanic Engineering*, vol. 27, no. 4, pp. 780–789, October 2002.

2. R. W. Sheriff, "Synthetic aperture beamforming with automatic phase compensation for high frequency sonars," in *Proceedings of the 1992 Symposium on Autonomous Underwater Vehicle Technology*. IEEE, 1992, pp. 236–245.

3. W. W. Bonifant, "Interferometric synthetic aperture sonar processing," Master's thesis, Georgia Institute of Technology, 1999.

4. W. E. Kock, "Extending the maximum range of synthetic aperture (hologram) systems," *Proceedings of the IEEE*, vol. 60, pp. 1459–1460, November 1972.

5. J. E. Dennis, *Numerical Methods for Unconstrained Optimization and Nonlinear Equations*. Prentice-Hall, Inc., 1983.

6. D. A. Cook, "Syntheic aperture sonar motion estimation and compensation," Master's thesis, School of Electrical and Computer Engineering, Georgia Institue of Technology, 2006.

7. J. W. Oeschger, "Estimating along-track dsiplacement using redundant phase centers," in *Proceedings of the Institute of Acoustics*, vol. 28, Pt. 5, 2006.

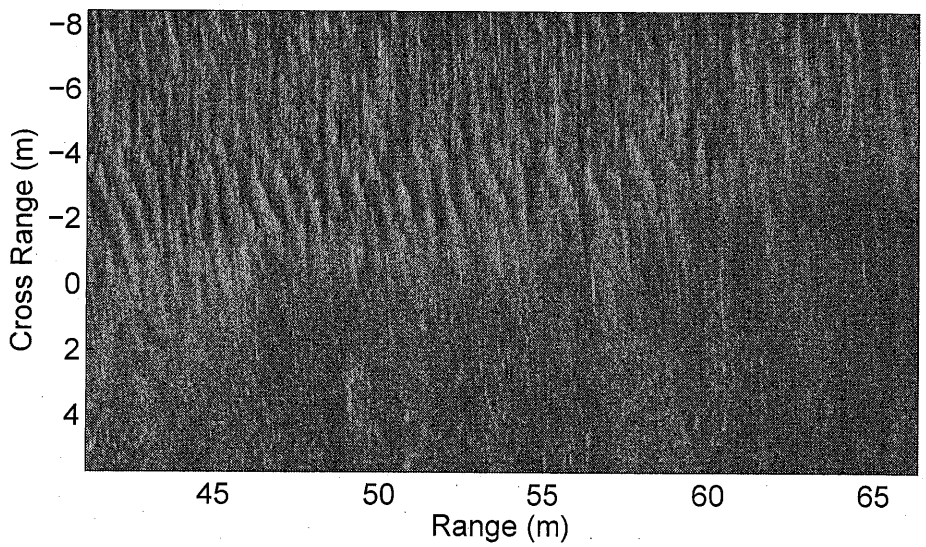

(a)

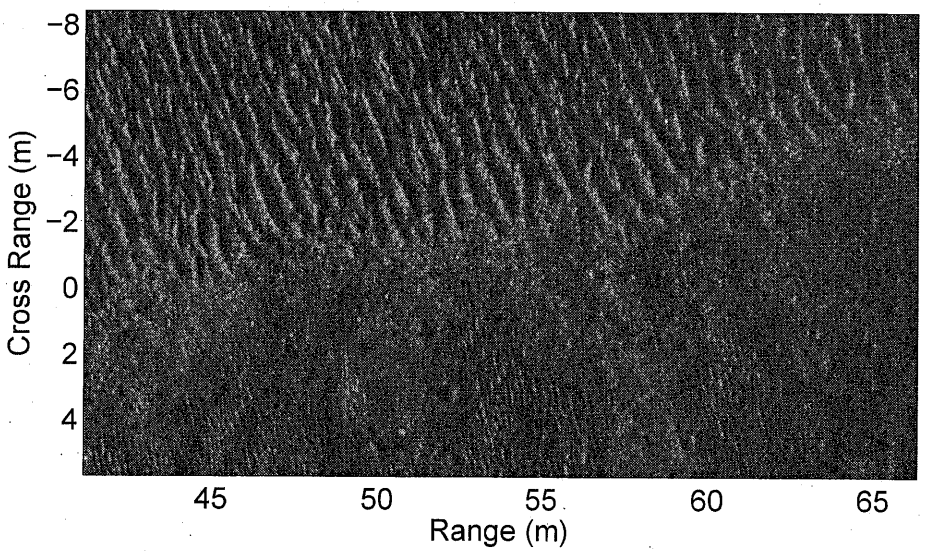

(b)

Figure 6: SAS image before (top) and after (bottom) motion compensation. Note the presence of both large and fine-scale sand ripples in (b).